LHH1, a Novel Antimicrobial Peptide with Anti-Cancer Activity Identified from *Lactobacillus casei* HZ1

Junfang He (HeJunfang2018@hotmail.com)
Tianjin University of Science and Technology https://orcid.org/0000-0001-6004-6009
Duxin Jin
Yangzhou University
Xuegang Luo
Tianjin University of Science and Technology
Tongcun Zhang
Tianjin University of Science and Technology

Original article

Keywords: Antimicrobial peptide, Anti-cancer, Lactobacillus casei, Staphylococcus aureus, Pathogenic bacteria

Posted Date: July 30th, 2020

DOI: https://doi.org/10.21203/rs.3.rs-44740/v1

Version of Record: A version of this preprint was published at AMB Express on November 11th, 2020. See the published version at https://doi.org/10.1186/s13568-020-01139-8.

Abstract

Antimicrobial peptides have been attracting increasing attention for their multiple beneficial effects. In present study, a novel AMP with a molecular weight of 1875.25 Da, was identified from the genome of *Lactobacillus casei* HZ1. The peptide, which was named as LHH1 was comprised of 16 amino acid residues, and its α-helix content was 95.34% when dissolved in 30 mM SDS. LHH1 exhibited a broad range of antimicrobial activities against gram-positive bacteria and fungus. It could effectively inhibit *staphylococcus aureus* with a minimum inhibitory concentration of 3.5 μM and showed a low hemolytic activity. The scanning electron microscope, confocal laser scanning microscope and flow cytometry results showed that LHH1 exerted its antibacterial activity by damaging the cell membrane of *staphylococcus aureus*. Meanwhile, LHH1 also exhibited anti-cancer activities against several cancer cells including MGC803, HCT116 and C666-1 cells, and one major action of its anti-cancer mechanism was breaking the cell membrane.

Introduction

Over the last decades, human health was seriously threatened by pathogenic bacteria-induced diseases. Antimicrobial drugs and chemical preservatives such as antibiotics, sulphonamides and 4-quinolones have been commonly used to protect human from the infections of pathogens. However, the overuse of antimicrobial drugs has led to drug-resistance in many strains of pathogenic bacteria and efficiency loss to inhibit pathogenic microorganisms (Alekshun and Levy 2007). What's worse, antibiotic drugs frequently affect normal human cells and posed a serious challenge to human health (McEwen and Collignon 2018). Thus, it's imperative to explore for natural, chemical preservative-free and safe antimicrobial alternatives.

Antimicrobial peptides (AMPs), which are generally comprised of 10–60 amino acid residues, have been commonly regarded as promising antibiotic alternatives with a broad-spectrum antimicrobial activity (Cheung and Otto 2018). As an evolutionarily ancient weapon to innate immunity, AMPs can protect human from invading pathogens such as bacteria, fungi, viruses and parasites (Mishra et al. 2017). Moreover, AMPs have been found in various species including multicellular plants, animals and microbiology (Aminov 2017). For example, LL-37 was isolated from a human bone marrow library (Gudmundur A. GUDMUNDSSON 1996), Leucocin A was a small heat-stable bacteriocin produced by *Leuconostoc gelidum* UAL187 (STILES 1995), γ-Purothionins was extracted from wheat endosperm (Colilla et al. 1990).

AMPs have been recognized as antimicrobial alternatives that overcome the limitations of current antibiotics, such as selective cytotoxicity for cancer cells and avoid the occurrence of multidrug-resistance. Recently, a growing evidence of studies have shown that some cationic AMPs exhibit a broad spectrum of cytotoxicity for cancer cells (Hoskin and Ramamoorthy 2008). Arpornsuwan et al. found that BmKn2 as an AMP showed inhibitory effect on colon carcinoma cells (Arpornsuwan et al. 2014), LL-37 and it's analogs exhibited anticancer effects on several cancer cell lines (Kuroda et al. 2015), human

intestinal defensin 5 could suppress the growth of colon cancer cells induced by 1,2-dimethylhydrazine dihydrochloride (Panjeta and Preet 2020).

Lactic acid bacterias are prebiotics that have been recognized as safe with a broad application in food and pharmaceutical industries. Moreover, it possesses the capability of producing AMPs (Pangsomboon et al. 2009). The first bacteriocin that completely identified from *Lactococcus lactis* was nisin, which has been acknowledged as safe by FDA (Food and Drug Administration) and approved for application in food industry (Paul D. Cotter 2005). Wen et al. reported that plantaricin K25 produced by *Lactobacillus plantarum* showed antibacterial activity against gram-positive and gram-negative bacteria (Wen et al. 2016). Meanwhile, pediocin and lacticin that produced by species of *Pediococcus* and *Lactococcus* have been permitted to use in food product (Kaya and Simsek 2019). Moreover, several AMPs such as Nisin Z and Plantaricin A from lactic acid bacteria have anticancer activity (Mulders et al. 1991, Nissen-Meyer et al. 1993). *Lactobacillus casei* (*L. casei*) HZ1 is also a species in lactic acid bacteria that separated from Chinese traditional fermented milk. Our previous study found a novel AMP (LGH2) from the genome of *L. casei* HZ1, which showed an excellent inhibitory activity against gram-positive bacteria (He et al. 2018). However, to our knowledge, only a few studies have been conducted on the antimicrobial and anticancer activities of AMPs from *L. casei*. Identification of more AMPs can provide structure templates for the production of antimicrobial and anticancer drugs. Hence, further research on AMPs from the genome of *L. casei* HZ1 is essential.

In the present study, we attempted to detect some novel AMPs with anti-cancer activity from the genome of *L. casei* HZ1, and to explore the functional mechanisms of the AMPs against pathogenic bacteria and cancer cells. The hemolytic activity was also characterized for cytotoxicity against red blood cells.

Materials And Methods

Identification of potential AMPs from the genome of L. casei HZ1

The prediction of AMPs from the genome of *L. casei* HZ1 was conducted according to our previous research with some modifications (He et al. 2018). Briefly, the prediction of antimicrobial peptides conforms to the following principles: (1) An AMP should contain a Gly-Gly/Ala leader motif at the front of N-terminal region of mature AMPs. (2) The peptide might form α-helix structure. (3) The peptide is positive-charged. (4) Protein-binding potential should be above 0 kcal/mol. The APD3 (http://aps.unmc.edu/AP/prediction/ prediction_main.php) was used to calculate the net charge, protein-binding potential and hydrophobic amino acid content in the peptide. The $CAMP_{R3}$ (http://www.camp.bicnirrh.res.in/prediction.php) was used to calculate the antibacterial capacity of the peptides. The molecular weight was calculated by PeptideMass (http://web.expasy.org/peptide_mass/). The secondary structure model was constructed by PSIPRED (http://bioinf.cs.ucl.ac.uk/psipred/). The hemolytic property of peptides was predicted by HemoPI (http://crdd.osdd.net/raghava/hemopi/

design.php) (Chaudhary et al. 2016). The genome of *L. casei* HZ1 was presented in the supplementary material.

Synthesis of the AMPs

The AMPs and FITC-labeled AMPs were chemically synthesized by Bootech Bioscience & Technology Co., Ltd. (Shanghai, China). The synthesized peptides were purified by reversed-phase high-performance liquid chromatography (RP-HPLC) and were verified by mass spectrometry.

Antimicrobial activity

The antimicrobial activity of AMPs was measured by inhibition zone assay. Briefly, 200 μL of pathogenic bacteria (5×10^6 CFU/mL) was added into 20 mL of Luria-Bertani (LB) solid medium and was spreaded evenly. Then, the round filter papers dampened with the AMPs were placed on the solid medium and were cultured at 37 °C for 18 h before recording the inhibition zones.

The minimun inhibitory concentration (MIC) was determined as described by Morita et al. with minor modifications (Morita et al. 2013). Briefly, the bacteria with a density of 1×10^6 cells/mL was added into a 96-well plate. Then, AMP solution was added into each well to reach a final concentration of 0 to 256 μM, and the plate was incubated at 37 °C for 24 h. The MIC value was determined by OD600 readings in a microplate reader (Infinite M200 PRO, TECAN, Switzerland).

For the assessment of the maximum kill concentration (MBC), 5 μL of each well culture was added into another 96 well plate which was filled with 95 μL of fresh nutrient broth in each well and was incubated at 37 °C for another 24 h. The absorbance was determined at 600 nm.

Hemolytic activity

The hemolytic activity was determined with goat red blood cell according to the method described by Taute et al. (Taute et al. 2015). Briefly, red blood cells were collected by centrifugation at 1000 × *g* for 10 min before washing thrice with 50 mM Tris-HCl and were resuspended with 50 mM Tris-HCl containing 100 mM NaCl to reach a final concentration of 4% (V/V). 200 μL of the goat red blood cells were mixed with LHH1 of different concentrations at 37 °C for 1 h. Then, the supernatant was collected by centrifugation at 1000 × *g* for 10 min, and 100 μL of the supernatant was transferred into a 96-well plate. The absorbance was monitored at 550 nm. PBS and 0.1% Trition X-100 solution were used to instead of AMP as negative and positive control, respectively.

$$\text{Hemolysis rate (\%)} = (A_{\text{Peptide}} - A_{\text{PBS}}) / (A_{\text{Triton}} - A_{\text{PBS}}) \times 100 \qquad (1)$$

Anticancer activity

HCT116 cell was cultured in 1640 medium with 10% (v/v) inactivated fetal bovine serum, while MGC803 and C666-1 cells were maintained in DMEM high glucose medium with 10% (v/v) inactivated fetal bovine

serum. All cells were cultured in an incubator containing 5% CO_2 at 37 °C and were harvested at 80% confluency. The cancer cells were plated at a density of 5×10^3 cells/well in 96-well culture dishes and were incubated with AMPs of different concentrations for 24 h. Then, 10 μL of MTT (5 mg/mL in PBS) was added into each well and was co-inculated at 37 °C for another 4 h. Subsequently, the precipitate was dissolved with DMSO after removing the medium, and the optical density was measured at 490 nm with a microplate reader.

Circular dichroismspectroscopy

The secondary structures of the peptides in different solutions were determined by a MOS-450 circular dichroism (CD) spectrometer (Bio-Logic, France) with a 0.5 cm quartz cell at 190–240 nm. The AMPs were dissolved in six solvents including water, sodium phosphate buffer (10 mM, pH 7.4), SDS micelles (30 mM), 25% TFE, 50% TFE and 500 mM phospholipid to a final concentration of 100 μM, respectively. An average of three scans was recorded for each sample. The acquired CD signal spectra was converted to the mean residue ellipticity. The secondary structures of the AMPs were calculated using the CD data at Dichroweb platform (http://dichroweb.cryst.bbk.ac.uk/html/links.shtml) using three different algorithms (SELCON3, CONTIN-LL and CDSSTR) (Whitmore and Wallace 2004).

Scanning electron microscopy

The morphology of *staphylococcus aureus* (*S. aureus*) was observed by scanning electron microscope (SEM). *S. aureus* at mid-logarithmic phase was harvested by centrifugation at 1000 × *g* at 4 °C for 10 min. The cells were diluted to a concentration of 1×10^8 CFU/mL with 10 mM PBS (pH 7.4). Then, *S. aureus* dilution was incubated with the AMPs for 30 min. After washing the bacteria three times with 10 mM PBS at 1000 × *g* for 10 min, the cells were resuspended in 2.5% glutaraldehyde for 30 min and were washed thrice with PBS. Then, the cells were dehydrated by 10%, 30%, 50%, 70%, 80%, 90% and 100% ethanol, respectively. The dehydrated cells were dried by CO_2 under critical point, and were sprinkled, gold-plated and imaged by SEM.

Flow cytometry

The effect of AMPs on cell membrane integrity of *S. aureus* was determinated by flow cytometry according to the method described by Xu, et al. (Xu et al. 2015). Briefly, *S. aureus* at mid-logarithmic phase was harvested by centrifugation at 1000 × *g* for 10 min, washed thrice with PBS and re-suspended the bacteria with PBS to a density of 1×10^6 cells/mL. Then, 300 μL of bacterial suspensions was mixed with 300 μL of AMPs to a final concentration of 10 μg/mL. The mixture was incubated at 37 °C for 1 h followed by dyeing with 20 μM propidium iodide (PI) in dark at 4 °C for 15 min. For control, PBS instead of the AMP was added. The mixture was detected by flow cytometer (C6, BD, USA).

The cancer cells were plated into 6-well culture plates (1×10^6 cells/well) and were treated with various concentrations of the AMP (5, 10, and 20 μg/mL) or untreated. After incubation for 1 h, the cells were harvested by tryptic digestion, washed thrice with cold PBS, and resuspended with 1 × binding buffer. 1 × 5 μL of FITC-conjugated Annexin V (BD

Bioscience, USA) and 5 μL of propidium iodide (PI) were added. The cells were gently mixed, and incubated at room temperature in dark for 15 min. After incubation, 400 μL of 1 × binding buffer was added to each tube, the stained cells were measured by flow cytometre.

Calcein leakage assay

The calcein-entrapped large unilamellar vesicle was prepared as described by Tang, et al. (Pu and Tang 2017). Briefly, 1-palmitoyl-2-oleoyl-sn-glycero-3-phosphoglycerol (POPG) and cardiolipin (CL) lipids were dissolved in chloroform, dried by nitrogen gas and were resuspended in dye buffer solution (10 mM HEPES, 50 mM calcein, pH 7.4). The suspension was subjected to 10 frozen-thaw cycles in liquid nitrogen and was extruded more than twenty times through polycarbonate filters with two stacked 100 nm pore size filters. Untrapped calcein was removed by Sephadex G-25 column. The leakage of calcein was detected by measuring the fluorescence intensity at an excitation wavelength of 490 nm and an emission wavelength of 515 nm in a microplate reader. The 100% dye leakage was determined by 1% Triton X-100. The percentage of dye leakage was calculated by the equation as follows.

$$\text{Dye leakage}\ (\%) = \frac{F - F_0}{F_{100} - F_0} \times 100 \qquad (2)$$

Where F_0 is the fluorescence intensity of liposomes without AMPs, F is the fluorescence intensity of liposomes treated with AMPs, F_{100} is the fluorescence intensity of liposomes treated with 1% Triton X-100.

Confocal laser scanning microscopy

S. aureus at mid-logarithmic phase was diluted to a concentration of 10^6 CFU/mL with PBS (pH7.4) and was co-incubated with labeled with fluorescein (FITC) synthetic peptide to reach a final concentration of 100 μM for 1 h. Then, the cells were washed thrice with PBS and were visualized with a confocal laser scanning microscope (CLSM) equipped with a Zeiss Neofluor × 40 objective (numerical aperture 0.75).

For cancer cells, 1×10^6 cancer cells were incubated with the optimal medium at 37 °C for 24 h. 10 mM FITC-labeled AMP was added and was co-cultured with the cells for 30 min before washing with PBS. Then, the cells were dyed with DAPI for another 10 min and were washed thrice with PBS. The cancer cells were observed using a CLSM at 40 × objective lens.

Statistical analysis

All experiments were carried out in thrice and the results were presented as the means ± standard deviation (SD) The data were analyzed with SPSS 19.0 and the level of significance were analyzed by one way analysis of variance (ANOVA). $p < 0.05$ were considered statistically significant.

Results

Prediction of AMPs from the genome of *L. casei* HZ1

To predict novel AMPs, the open reading frames (ORF) that less than 450 bps in the genome of *L. casei* HZ1 were analyzed. Four novel potential AMPs were obtained and were blasted by NCBI and APD3 data bank, which showed that these four peptides had not been reported. The characteristics of the four AMPs were listed in Table 1. The four putative AMPs displayed a low hemolytic score, which indicated that they were low toxic. However, hydrophobic rate and helix contents of the four AMPs were obviously different. Compared with other three peptides, LHH1 contained a relatively high hydrophobic amino acid and helix content with a HR value and helix content of 62% and 81.25%, respectively. Moreover, LHH1 possessed the highest pI value of 11.71 and the lowest molecular weight of 1875.25 Da compared to other three peptides. As shown in Table 2, both LHH1 and LHH4 shared the same motif of Gly-Gly at the N-terminus of the predicted AMPs, while LHH2 and LHH3 had the same motif of Gly-Ala at the N-terminus of the predicted AMPs.

Table 1
The characteristics of the four peptides.

Name	Amino acid sequence	pI	NC	NA	HR	Helix	HS	MW
LHH1	AFALIAGALYRIFHRR	11.70	+ 3	16	62	81.25	0.49	1875.25
LHH2	EKAPEAYVKKIASLYRNKRY	9.87	+ 4	20	30	75.00	0.49	2427.82
LHH3	LIQFLEDNKKTTPHANAK	8.51	+ 1	18	33	31.25	0.51	2068.36
LHH4	FGVIVGHCLGHSGNWRKWIE	8.24	+ 1	20	45	15.00	0.48	2295.65

Net charge (NC) represents the total charge of an AMP; Number of amino acid residues (NA) is the total number of amino residues in the peptide; Hydrophobic rate (HR) is the rate of hydrophobic amino acids in the sequence of AMP, %; Helix is the content of helix structure in the secondary structure of AMPs, %. Hemolytic score (HS) indicates the hemolytic potency.

Table 2
The location of the four peptides precursor in the genome of *L .casei* HZ1

Name	Peptide precursor	Location in *L. case* HZ1
LHH1	$(Aa)_{50}$ GG AFALIAGALYRIFHRR	LSEI_2135
LHH2	$(Aa)_{38}$ GA EKAPEAYVKKIASLYRNKRY	LSEI_1186
LHH3	$(Aa)_{28}$ GA LIQFLEDNKKTTPHANAK	LSEI_1507
LHH4	$(Aa_{)8}$ GG FGVIVGHCLGHSGNWRKWIE	LSEI_0501

Antimicrobial activity of the four putative AMPs

To test antimicrobial activities of the four predicted AMPs, an inhibition zone assay was applied to analyze the antimicrobial activities against several bacterial strains including *S. aureus*, *L. monocytogenes*, *K. pneumoniae* and *E. aerogenes*. Compared to the other three peptides, LHH1 had the

antimicrobial activities with an obvious inhibition zone (Fig. 1). However, other three AMPs showed no inhibitory effect against the tested pathogenic bacteria.

To further explore the antimicrobial activity of LHH1, inhibitory effect of LHH1 on eight strains including two fungus, four Gram-positive bacteria and two Gram-negative bacteria were evaluated in this study (Table 3). The results showed that LHH1 exhibited better inhibitory effect on several bacterial strains involving *S. aureus*, *M. luteus*, *L. monocytogenes* and *P. pastoris* GS115, all of which belonged to Gram-positive bacteria and fungus. The present results displayed that LHH1 possessed the strongest antimicrobial activity against Gram-positive bacteria, especially against *S. aureus* with a MIC value of 3.5 μM. Meanwhile, LHH1 exerted a weak inhibition on *L. casei*, which is a prebiotics that beneficial to human health.

Table 3
Antimicrobial activity of LHH1.

Microbial Strains	LHH1		Ampicillin	
	MIC (μM)	MBC (μM)	MIC (μM)	MBC (μM)
Gram-				
Enterobacter aerogenes (ATCC 13048)	> 256	> 256	8.00	16.00
Klebsiella pneumoniae (ATCC 700603)	> 256	> 256	4.00	8.00
Gram+				
Staphylococcus aureus (ATCC 29213)	3.50	6.50	0.25	0.50
Micrococcus luteus (ATCC 14452)	7.50	14.00	0.125	0.25
Listeria monocytogenes (ATCC 7611)	8.00	15.50	0.125	0.25
Lactobacillus casei (ATCC334)	> 256	> 256	0.5	1.0
Fungus				
Saccharomyces cerevisiae (ATCC 204508)	32.00	64.00	—	—
Pichia pastoris GS115 (ATCC 20864)	16.00	32.00	—	—

Hemolytic activity of LHH1

To confirm whether LHH1 was safe or not, its hemolytic activity was assessed. As showed in Fig. 2, LHH1 showed a low hemolytic activity against goat red blood cell when its concentration was lower than 64 μM. However, an obvious hemolysis was observed when its concentration was higher than 128 μM. The HC_{50} (hemolytic rate of 50%) value of LHH1 was 187.2 μM. The hemolysis results indicated that LHH1 exhibited an excellent inhibitory action on several Gram-positive bacteria at a low hemolytic concentration.

Dye leakage assays

Calcein leakage assay is a common method to identify whether AMPs could interact with the phospholipids or not (Domingues et al. 2015). POPG and CL were two major cell membrane phospholipids of *S. aureus*, while calcein can be entrapped in LUV composed of CL/POPG (42:58) (Richard M. Epand 2008, Lohner and Prenner 1999). If AMPs could interact with the phospholipids, the LUV would be damaged before the leakage of calcein. As shown in Fig. 3, calcein leakage ratio displayed a dose-dependent increasing manner. LHH1 induced a calcein leakage content of over 50% at a concentration of higher than 15 μM. The calcein leakage results indicated that LHH1 could lead to the damage of phospholipid membrane of *S. aureus*.

Secondary structure analysis of LHH1

CD spectra has been considered as a powerful and sophisticated technique to analyze the secondary structure of protein (M. HOLLOSI 1994). Secondary structure of LHH1 dissolved in six different solutions was detected by CD spectra, and the results were shown in Fig. 4 and Table 4. LHH1 showed two obvious two negative peaks at 208 nm and 220 nm and a positive peak at 192 nm respectively when it was dissolved in 30 mM SDS, 25% TFE, 50% TFE and 500 μM (CL:PG), which were the typical characteristics of α-helical structure in the peptides. However, LHH1 showed a relatively flat curve when it was dissolved in H_2O and PBS. The contents of secondary structures of LHH1 in different solvents were determined by SELCON3 program. As shown in Table 4, LHH1 showed a high α-helix content of 95.29% and 95.34% when it dissolved in 50% TFE and 30 mM SDS, respectively. Meanwhile, α-helical contents of LHH1 in 500 μM CL: PG (42:58) was 73.05%. However, LHH1 mainly presented a structure of random coil when it dissolved in water.

Table 4
Contents of secondary structures of LHH1 in different solvents.

Solvent	Alpha-helix (%)	Beta-sheet (%)	Random coil (%)
Water	16.70 ± 2.50	4.85 ± 1.70	84.35 ± 3.10
PBS	47.48 ± 3.80	1.73 ± 0.70	52.57 ± 2.90
30 mM SDS	95.34 ± 3.10	0.02 ± 0.00	19.64 ± 1.50
TFE 25%	87.32 ± 3.70	0.04 ± 0.00	12.91 ± 0.00
TFE 50%	95.29 ± 3.0	0.02 ± 0.00	5.50 ± 0.40
500 μM (CL:PG)	73.05 ± 2.80	0.26 ± 0.04	26.69 ± 0.60

Membrane damage induced by LHH1

To explore whether LHH1 could bind to cell membrane of *S. aureus* or not, antibacterial mechanism of LHH1 against *S. aureus* was further studied by CLSM. As showed in Fig. 5, the fluorescence signal was obviously observed on the surface of *S. aureus*, when it was treated with FITC-labeled LHH1, which indicated that LHH1 could bind to the cell membrane of *S. aureus*.

To further confirm whether LHH1 could induce the membrane damage of *S. aureus*, SEM was utilized to observe the morphology of bacterial cells. *S. aureus* showed a smooth and intact surface (Fig. 6A). However, LHH1 induced a roughened and deformed changes on the membrane of *S. aureus* at a dose-dependent manner. Meanwhile, *S. aureus* was covered with blebs, and some deformed and collapsed cells were observed when it was exposed to LHH1 of 0.5 × MIC or 1.0 × MIC (Fig. 6B-C).

To further explore the effect of LHH1 on membrane integrity of *S. aureus*, DNA intercalating PI was applied in this study. PI could penetrate into the cell and stain the nucleic acids if the membrane was damaged. As shown in Fig. 7, S. *aureus* showed no fluorescence when it was not treated with LHH1. However, the cells displayed a PI fluorescent signal after the treatment of LHH1, and the fluorescence intensity was positively correlated with the concentration of LHH1. LHH1 of 2 × MIC could cause approximately 97.2% cells of *S. aureus* stained by PI. Flow cytometry results indicated that LHH1 could induce the membrane damage of *S. aureus*.

Anticancer activity of LHH1

Anticancer activities of LHH1 were evaluated by MTT assays. Cell viability results were depicted in Fig. 8. LHH1 could dose-dependently inhibit the viabilities of C666-1, MGC803 and HCT116 cells. LHH1 exhibited the strongest inhibitory effect on C666-1 cells with an IC_{50} value of 19 μM, while its IC_{50} values of inhibiting MGC803 and HCT116 cells were 32 μM and 41 μM, respectively.

Anticancer action of LHH1

To explore whether LHH1 had an influence on the membranes of cancer cells or not, three cancer cells were treated with FITC-labeled LHH1 and were observed with CLSM. As presented in Fig. 9, LHH1 could bind with the membranes of the three cancer cells, and the morphology of the cancer cells became blurred. Meanwhile, LHH1 could penetrate into the membranes of the three cancer cells.

To further clarify the mechanisms of inhibitory effects of LHH1, the three cancer cells were stained with Annexin V-FITC/PI and were analyzed by flow cytometry. As showed in Fig. 10, LHH1 dose-dependently induced an increasing accumulation of apoptotic cells for all the three measured cancer cells, while LHH1 mainly induced a late apoptosis. At 20 μM, LHH1 induced late apoptotic rates of 18.1%, 21.0% and 26.1% for MGC803, HCT116 and C666-1 cells, respectively. Moreover, small amounts of early apoptotic cells were observed for different cancer cells.

Discussion

AMPs have been recognized as the first line of defence against pathogens infection, and a growing body of evidence suggested that some bactericidal peptides showed anticancer and antiviral activities (Jiang et al. 2020). In the present study, LHH1 was a novel AMP that identified from the genome of *L. casei* HZ1 with potent bactericidal effect on *S. aureus* and anticancer potency on several cancer cells (Table 3 and Fig. 8), which may provide clear evidence for the application of LHH1 in certain foods as preservatives. Currently, there are 43 AMPs origined from *Lactobacillus* and 25 AMPs from *Lactococcus*, while only nisin and pediocin PA-1 are considered as potent bio-preservatives applied in food industry (Vijay Simha et al. 2012). The hemolytic property is an important criteria for evaluating the security of AMP as an additive agent or a drug. LHH1 in this study showed a low hemolytic activity at its effective antibacterial activity (Table 3 and Fig. 2).

Many class II bacteriocins produced by LAB are synthesized as precursors containing a Gly-Gly/Ala motif leader sequence. The presence of a Gly-Gly/Ala motif containing peptide is closely related to the presence of a dedicated ATP-binding cassette (ABC) transporter (Dirix et al. 2004). Most of the prepeptides belonging to the class II AMPs, contain a Gly-Gly/Ala motif leader sequence that are recognized and removed by their cognate ABC-transporter (van Belkum et al. 1997, Patton et al. 2008). The precursor of LHH1 contains 68 amino acid residues, while Gly-Gly motif was involved in its leader sequence. These characteristics are suitable for a protein expression by ABC-transporter from *L. casei* HZ1.

The structural characteristics of AMPs play critical roles in their antimicrobial activity. Most of the bacteriocins found in LABs were defined as cationic polypeptides. The postive-charged LHH1 could specifically kill Gram-positive bacteria rather than Gram-negative bacteria, which may result from the differences in the composition of bacterial lipid membranes. For example, the lipid membranes of *S. aureus* mainly consisted of negatively charged lipid such as cardiolipin (CL) and phosphatidylglycerol (PG), whereas the lipid membranes of Gram-negative bacteria (ie. *E. coli*) were uncharged phosphatidylethanolamine (Richard M. Epand 2008, Lohner and Prenner 1999). The selective bacterial cytotoxicity of cationic AMPs could be partly attributed to the net negative charge on the bacterial cell membranes, which facilitated the positive charges specifically target the negative-charged phospholipids on the membranes of Gram-positive bacteria (Arpornsuwan et al. 2014, Fields et al. 2018). Moreover, the increased net positive charge on the peptide might increase the binding affinity and stabilize the amphiphilic structure on the negative-charged lipid membrane (Ahn et al. 2006). A high proportion of positively charged amino acids at the C-terminus of LHH1 was speculated to play a pivotal role in the antimicrobial action for their cationic property. LHH1 has a similar residue of R-R/K with Pep27, Chrysophsin-1 and TP4 in the C-terminus of AMPs (Fig. 11). Arg residues was highlighted in previous researches for its critical role in the antimicrobial activity, which endow the peptides with cationic charges and hydrogen bonding properties necessary for interaction with the abundant anionic components of bacterial membrane (Chan et al. 2006). LHH1 possessed the capacity of binding with the cell membrane of bacteria and cancer (Fig. 5 and Fig. 9). The present results were in accordance with previous researches that positive-charged amino acids in AMPs were required for binding to the negative-charged membrane through electrostatic interaction (Wimley 2010).

Hydrophobicity is a factor that plays pivotal roles in generating α-helix structure, and it is positively correlated with the membrane disrupting power of the peptides to a certain extent (Mattei et al. 2014, Ng and Deber 2014). In this study, 211 APMs with the anticancer activities, which were collected by APD3, were blasted with LHH1 to analyze the peptide sequence similarity. Three AMPs had the highest sequence similarity with LHH1, they were Pep27, Chrysophsin-1 and TP4 (Fig. 11). LHH1 has the highest rate of hydrophobic amino acid among the four AMPs. The hydrophobic amino acid rate of LHH1, Pep27, Chrysophsin-1 and TP4 are 62%, 29%, 48% and 44%. The sequence fragment of AFALIAGAL at the N-terminus of LHH1 contained a high proportion of hydrophobic amino acids. Generally, increased hydrophobicity of the non-polar face of an amphipathic α-helical peptide could improves antimicrobial activities (Dathe et al. 1997). As reported by Mattei, et al., hydrophobicity is positively correlated with the membrane disrupting power of the peptides to a certain extent (Bluhm et al. 2015).

α-Helical conformation in AMPs is equally crucial in determining the antimicrobial activity of AMPs. Our present results showed that the α-helical content of LHH1 increased to above 85% when it was encountered with TFE and SDS micelle environment (Fig. 4 and Table 4), which indicated that LHH1 was an α-helix AMP. As α-helical structure could enhance the permeabilization of AMPs into the membrane of *S. aureus* (Park et al. 2004), it might play a significant role in the antimicrobial effectiveness of LHH1. The high content of α-helix structure will facilitate the formation of holes in the cell membrane of *S. aureus*, thus causing leakage of cytoplasm from the cell and inhiniting the growth of *S. aureus* (Park et al. 2004). Juba et al. reported that α-helix in AMPs could specifically interfere with the phospholipid fluidity, form a transient hole on the membrane and disrupt the membrane of *S. aureus*, thus inducing cytoplasmic membrane permeabilization and improving the antimicrobial activity (Juba et al. 2015). In this study, calcein leakage assay confirmed the interaction between LHH1 and the phospholipids on membrane of *S. aureus* (Fig. 3). In the present study, scanning electron microscope, confocal laser scanning microscope and flow cytometer were used to analyse the influence of LHH1 on *S. aureus*. The membrane of *S. aureus* was obviously disrupted after the treatment of LHH1 (Fig. 5–7), which provided distinct evidence that the major antimicrobial action of LHH1 was interacting with phospholipids, damaging the membrane of *S. aureus* through its helix-forming amphipathic structure and resulting in the leakage of cytoplasm. Furthermore, glycine in the sequence of LHH1 was positioned between hydrophobic amino acid and cationic amino acid fragments, which made the folding and distortion of secondary structure of LHH1 be available and was structurally beneficial for the inhibitory action of LHH1 against *S. aureus* (Rajeev Aurora 1994, Huang et al. 2014).

Antimicrobial peptides have been commonly considered to cause cancer cells to undergo rapid cell death through a direct cell membrane damaging effect. Variation in the composition of cell membrane has significant implications in the progression of cancer. Cancer cell membrane presented more negative charge and stronger membrane fluidity on cell membrane than normal cells. Thus, destroying the cell membrane of cancer cells could be an effective strategy to inhibit the growth of cancer cells. Our anti-cancer results confirmed that cationic AMPs could specifically induce the apoptosis of several cancer cells including MGC803, HCT116 and C666-1 cells (Fig. 8). LHH1 exerted its anticancer activity partly by

ult showed that Annexin-V could interact with

the phosphatidylserine (PS), which indicated that the membrane of cancer cells was damaged by LHH1 (Fig. 10). Thus, electrostatic interactions between cationic LHH1 and negatively charged components in membrane of cancer cells may be vital in selective disrupting the membrane of the three detected cancer cells. As reported by Gaspar et al., anticancer activity of AMPs is mainly attributed to the electrostatic interactions between the peptides and the anionic membrane of cancer cells, and allow selective killing cancer cells (Gaspar et al. 2013).

In conclusion, LHH1 as a novel AMP that identified from the genome of *L. casei* HZ1, possessed a broad spectrum of antimicrobial and anticancer activities and its effective concentration was under low toxicity. Meanwhile, the present results indicated that the major antimicrobial and anticancer actions of LHH1 were via damaging cell membranes.

Declarations

Authors' contributions

He JF participated in research design. He JF and Jin DX were responsible for performing the experiments and data analysis. He JF wrote the manuscript, He JF, Jin DX, Luo XG and Zhang TC contributed to the writing and editing of the manuscript.

Author details

[1] College of Biotechnology, Tianjin University of Science and Technology, Tianjin, 300457, P. R. China. [2] School of Food Science and Engineering, Yangzhou University, Yangzhou, Jiangsu, 225127, China.

Funding

This study was was funded by the National Key R&D Program of China (2017YFD0400303), the Natural Science Foundation of Tianjin (18JCZDJC33800), the Innovative Research Team of Tianjin Municipral Education Commission (NO. TD13-5015), the Young Teachers' Innovation Fund of Tianjin University of Science and Technology (NO. 2016LG06) and the Project for the Public Service Platform of Strain Breeding and Fermentation Technology of Industrial Microorganisms (17PTGCCX00190).

Acknowledgments

We thank the reviewers for their great comments.

Competing interests

The authors declare that they have no competing interests.

Availability of data and materials

Please contact author for data requests.

Ethics approval and consent to participate

Not applicable.

Consent for publication

Not applicable.

References

Ahn HS, Cho W, Kang SH, Ko SS, Park MS, Cho H, Lee KH (2006) Design and synthesis of novel antimicrobial peptides on the basis of alpha helical domain of Tenecin 1, an insect defensin protein, and structure-activity relationship study. Peptides 27(4): 640-8. https://doi.org/10.1016/j.peptides.2005.08.016

Alekshun MN, Levy SB (2007) Molecular mechanisms of antibacterial multidrug resistance. Cell 128(6): 1037-50. https://doi.org/10.1016/j.cell.2007.03.004

Aminov R (2017) History of antimicrobial drug discovery: Major classes and health impact. Biochem Pharmacol 133: 4-19. https://doi.org/10.1016/j.bcp.2016.10.001

Arpornsuwan T, Sriwai W, Jaresitthikunchai J, Phaonakrop N, Sritanaudomchai H, Roytrakul S (2014) Anticancer activities of antimicrobial BmKn2 peptides against oral and colon cancer cells. Int J Pept Res Ther 20(4): 501-509. https://doi.org/10.1007/s10989-014-9417-9

Bluhm ME, Knappe D, Hoffmann R (2015) Structure-activity relationship study using peptide arrays to optimize Api137 for an increased antimicrobial activity against Pseudomonas aeruginosa. Eur J Med Chem 103: 574-82. https://doi.org/10.1016/j.ejmech.2015.09.022

Chan DI, Prenner EJ, Vogel HJ (2006) Tryptophan- and arginine-rich antimicrobial peptides: structures and mechanisms of action. Biochim Biophys Acta 1758(9): 1184-202. https://doi.org/10.1016/j.bbamem.2006.04.006

Chaudhary K, Kumar R, Singh S, Tuknait A, Gautam A, Mathur D, Anand P, Varshney GC, Raghava GP (2016) A web server and mobile app for computing hemolytic potency of peptides. Sci Rep 6: 22843. https://doi.org/10.1038/srep22843

Cheung GY, Otto M (2018) Do antimicrobial peptides and antimicrobial-peptide resistance play important roles during bacterial infection. Future microbiology 13(10): 1073-1075.

Colilla FJ, Rocher A, Mendez E (1990) Gamma-Purothionins: amino acid sequence of two polypeptides of a new family of thionins from wheat endosperm. FEBS Letters 270(1-2): 191-194. https://doi.org/10.1016/0014-5793(90)81265-p

Dathe M, Wieprecht T, Nikolenko H, Handel L, Maloy WL, MacDonald DL, Beyermann M, Bienert M (1997) Hydrophobicity, hydrophobic moment and angle subtended by charged residues modulate antibacterial and haemolytic activity of amphipathic helical peptides. FEBS Letters 403(2): 208-212. https://doi.org/10.1016/s0014-5793(97)00055-0

Dirix G, Monsieurs P, Dombrecht B, Daniels R, Marchal K, Vanderleyden J, Michiels J (2004) Peptide signal molecules and bacteriocins in Gram-negative bacteria: a genome-wide in silico screening for peptides containing a double-glycine leader sequence and their cognate transporters. Peptides 25(9): 1425-1440. https://doi.org/10.1016/j.peptides.2003.10.028

Domingues TM, Perez KR, Miranda A, Riske KA (2015) Comparative study of the mechanism of action of the antimicrobial peptide gomesin and its linear analogue: The role of the beta-hairpin structure. Biochim Biophys Acta 1848(10 Pt A): 2414-21. https://doi.org/10.1016/j.bbamem.2015.07.012

Fields FR, Carothers KE, Balsara RD, Ploplis VA, Castellino FJ, Lee SW (2018) Rational design of syn-safencin, a novel linear antimicrobial peptide derived from the circular bacteriocin safencin AS-48. J Antibiot 71(6): 592-600. https://doi.org/10.1038/s41429-018-0032-4

Gaspar D, Veiga AS, Castanho MA (2013) From antimicrobial to anticancer peptides. A review. Front Microbiol, 4: 294. https://doi.org/10.3389/fmicb.2013.00294

Gudmundur HG, Birgitta A, Jacob O, Tomas B, Berit O, Rosalba S (1996) The human gene FALL39 and processing of the cathelin precursor to the antibacterial peptide LL-37 in granulocytes. Eur J Biochem 238(2): 325-332.

He JF, Luo XG, Jin DX, Wang YY, Zhang TC (2018) Identification, recombinant expression, and characterization of LGH2, a Novel Antimicrobial Peptide of *Lactobacillus casei* HZ1. Molecules 23(9). https://doi.org/10.3390/molecules23092246

Hoskin DW, Ramamoorthy A (2008) Studies on anticancer activities of antimicrobial peptides. Biochim Biophys Acta 1778(2): 357-75. https://doi.org/10.1016/j.bbamem.2007.11.008

Huang Y, He L, Li G, Zhai N, Jiang H, Chen Y (2014) Role of helicity of alpha-helical antimicrobial peptides to improve specificity. Protein Cell 5(8): 631-42. https://doi.org/10.1007/s13238-014-0061-0

Jiang Y, Wu Y, Wang T, Chen X, Zhou M, Ma C, Xi X, Zhang Y, Chen T, Shaw C, Wang L (2020) Brevinin-1GHd: a novel Hylarana guentheri skin secretion-derived Brevinin-1 type peptide with antimicrobial and anticancer therapeutic potential. Biosci Rep 40(5). https://doi.org/10.1042/BSR20200019

Juba ML, Porter DK, Williams EH, Rodriguez CA, Barksdale SM, Bishop BM (2015) Helical cationic antimicrobial peptide length and its impact on membrane disruption. Biochim Biophys Acta 1848(5): 1081-91. https://doi.org/10.1016/j.bbamem.2015.01.007

Kaya HI, Simsek O (2019) Characterization of pathogen-specific bacteriocins from lactic acid bacteria and their application within cocktail against pathogens in milk. Lwt-Food Sci Technol 115: 108464. https://doi.org/10.1016/j.lwt.2019.108464

Kuroda K, Okumura K, Isogai H, Isogai E (2015) The human cathelicidin antimicrobial peptide LL-37 and mimics are potential anticancer drugs. Front Oncol 5: 144. https://doi.org/10.3389/fonc.2015.00144

Lohner K, Prenner EJ (1999) Differential scanning calorimetry and X-ray diffraction studies of the specificity of the interaction of antimicrobial peptides with membrane-mimetic systems. Biochim Biophys Acta 1462(1-2): 141-56. https://doi.org/10.1016/s0005-2736(99)00204-7

Hõllosi M, Majer ZS, Rónai AZ, Magyar A, Medzihradszky K, Holly S, Perczel A, Fasman GD (1994) CD and fourier transform IR spectroscopic studies of peptides. II. detection of β-turns in linear peptides. Biopolymers 34(2): 177-185.

Mattei B, Miranda A, Perez KR, Riske KA (2014) Structure-activity relationship of the antimicrobial peptide gomesin: the role of peptide hydrophobicity in its interaction with model membranes. Langmuir 30(12): 3513-3521. https://doi.org/10.1021/la500146j

McEwen SA, Collignon PJ (2018) Antimicrobial resistance: a one health perspective. Microbiol Spectr 6(2). https://doi.org/10.1128/microbiolspec.ARBA-0009-2017

Mishra B, Reiling S, Zarena D, Wang G (2017) Host defense antimicrobial peptides as antibiotics: design and application strategies. Curr Opin Chem Biol 38: 87-96. https://doi.org/10.1016/j.cbpa.2017.03.014

Morita S, Tagai C, Shiraishi T, Miyaji K, Iwamuro S (2013) Differential mode of antimicrobial actions of arginine-rich and lysine-rich histones against Gram-positive *Staphylococcus aureus*. Peptides 48: 75-82. https://doi.org/10.1016/j.peptides.2013.07.025

Mulders JW, Boerrigter IJ, Rollema HS, Siezen RJ, de Vos WM (1991) Identification and characterization of the lantibiotic nisin Z, a natural nisin variant. Eur J Biochem 201(3): 581-4. https://doi.org/10.1111/j.1432-1033.1991.tb16317.x

Ng DP, Deber CM (2014) Terminal residue hydrophobicity modulates transmembrane helix-helix interactions. Biochemistry 53(23): 3747-57. https://doi.org/10.1021/bi500317h

Nissen-Meyer J, Larsen AG, Sletten K, Daeschel M, Nes IF (1993) Purification and characterization of plantaricin A, a *Lactobacillus plantarum* bacteriocin whose activity depends on the action of two peptides. J Gen Microbiol 139(9): 1973-8. https://doi.org/10.1099/00221287-139-9-1973

Pangsomboon K, Bansal S, Martin GP, Suntinanalert P, Kaewnopparat S, Srichana T (2009) Further characterization of a bacteriocin produced by *Lactobacillus paracasei* HL32. J Appl Microbiol 106(6): 1928-40. https://doi.org/10.1111/j.1365-2672.2009.04146.x

Panjeta A, Preet S (2020) Anticancer potential of human intestinal defensin 5 against 1, 2-dimethylhydrazine dihydrochloride induced colon cancer: A therapeutic approach. Peptides, 126: 170263. https://doi.org/10.1016/j.peptides.2020.170263

Park IY, Cho JH, Kim KS, Kim YB, Kim MS, Kim SC (2004) Helix stability confers salt resistance upon helical antimicrobial peptides. J Biol Chem 279(14): 13896-901. https://doi.org/10.1074/jbc.M311418200

Patton GC, Paul M, Cooper LE, Chatterjee C, van der Donk WA (2008) The importance of the leader sequence for directing lanthionine formation in lacticin 481. Biochemistry, 47(28): 7342-51. https://doi.org/10.1021/bi800277d

Cotter PD, Hill C, Ross, RP (2005) Bacteriocins: Developing innate immunity for food. Nat Rev Microbiol, 3(10): 777-788. https://doi.org/doi:10.1038/nrmicro1240

Pu C, Tang W (2017) Affinity and selectivity of anchovy antibacterial peptide for Staphylococcus aureus cell membrane lipid and its application in whole milk. Food Control 72: 153-163. https://doi.org/10.1016/j.foodcont.2016.08.009

Aurora R, Srinivasan R, Rose GD (1994) Rules for α-helix termination by glycine. Science 264(5162): 1126-1130.

Epand RM, Rotem S, Mor A, Berno B, Epand RF (2008) Bacterial membranes as predictors of antimicrobial potency. J Am Chem Soc 130(43): 14346–14352.

van Belkum MJ, Stiles ME (1995) Molecular characterization of genes involved in the production of the bacteriocin leucocin A from Leuconostoc gelidurn. Appl Environ Microb, 61(10): 3573–3579.

Taute H, Bester MJ, Neitz AW, Gaspar AR (2015) Investigation into the mechanism of action of the antimicrobial peptides Os and Os-C derived from a tick defensin. Peptides 71: 179-87. https://doi.org/10.1016/j.peptides.2015.07.017

van Belkum MJ, Worobo RW, Stiles ME (1997) Double-glycine-type leader peptides direct secretion of bacteriocins by ABC transporters: colicin V secretion in *Lactococcus lactis*. Mol Microbiol 23(6): 1293-301.

Vijay Simha B, Sood SK, Kumariya R, Garsa AK (2012) Simple and rapid purification of pediocin PA-1 from *Pediococcus pentosaceous* NCDC 273 suitable for industrial application. Microbiol Res 167(9): 544-9. https://doi.org/10.1016/j.micres.2012.01.001

Wen LS, Philip K, Ajam N (2016) Purification, characterization and mode of action of plantaricin K25 produced by *Lactobacillus plantarum*. Food Control 60: 430-439. https://doi.org/10.1016/j.foodcont.2015.08.010

Whitmore L, Wallace BA (2004) Dichroweb, an online server for protein secondary structure analyses from circular dichroism spectroscopic data. Nucleic Acids Res 32: W668-73. https://doi.org/10.1093/nar/gkh371

Wimley WC (2010) Describing the mechanism of antimicrobial peptide action with the interfacial activity model. ACS Chem Biol 5(10): 905-17. https://doi.org/10.1021/cb1001558

Xu L, Chou S, Wang J, Shao C, Li W, Zhu X, Shan A (2015) Antimicrobial activity and membrane-active mechanism of tryptophan zipper-like beta-hairpin antimicrobial peptides. Amino Acids 47(11): 2385-97. https://doi.org/10.1007/s00726-015-2029-7

Supplementary Materials

The following are available online. Figures S1–S10 show RP-HPLC and MS of the chemically synthesized peptides LHH1, LHH2, LHH3, LHH4 and FITC-LHH1, respectively. Figure S11 is a schematic diagram of FITC-LHH1 fluorescein labeling.

Figures

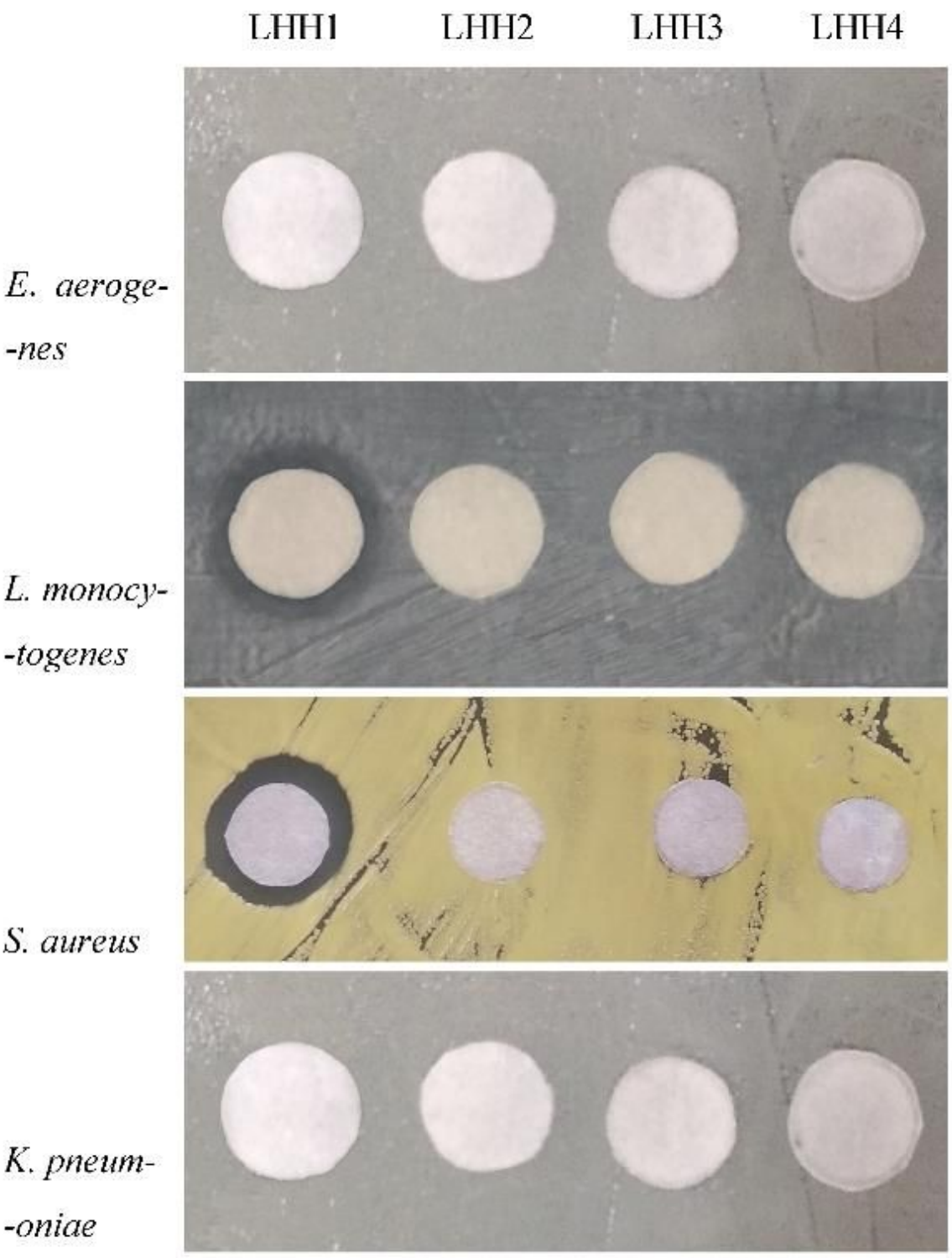

Figure 1

Inhibition zones of the four AMPs against several pathogenic bacteria.

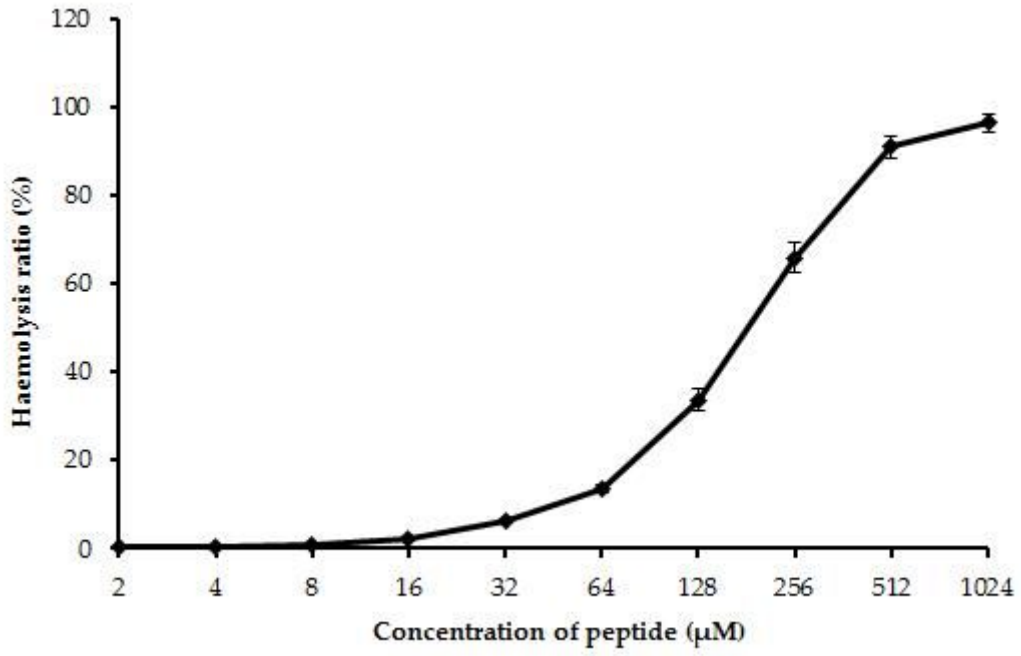

Figure 2

Hemolytic activity of LHH1.

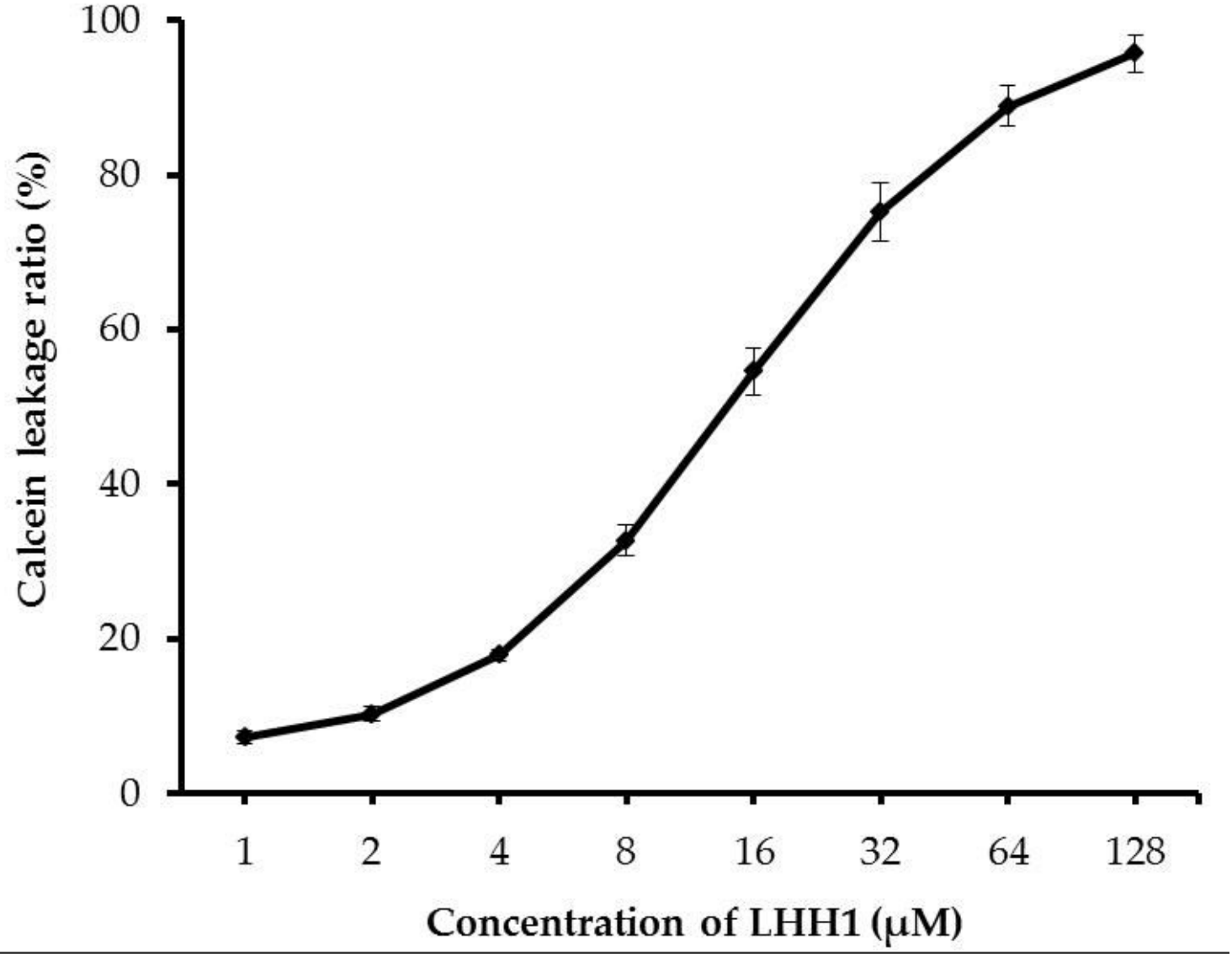

Figure 3

Release of calcein from liposomes.

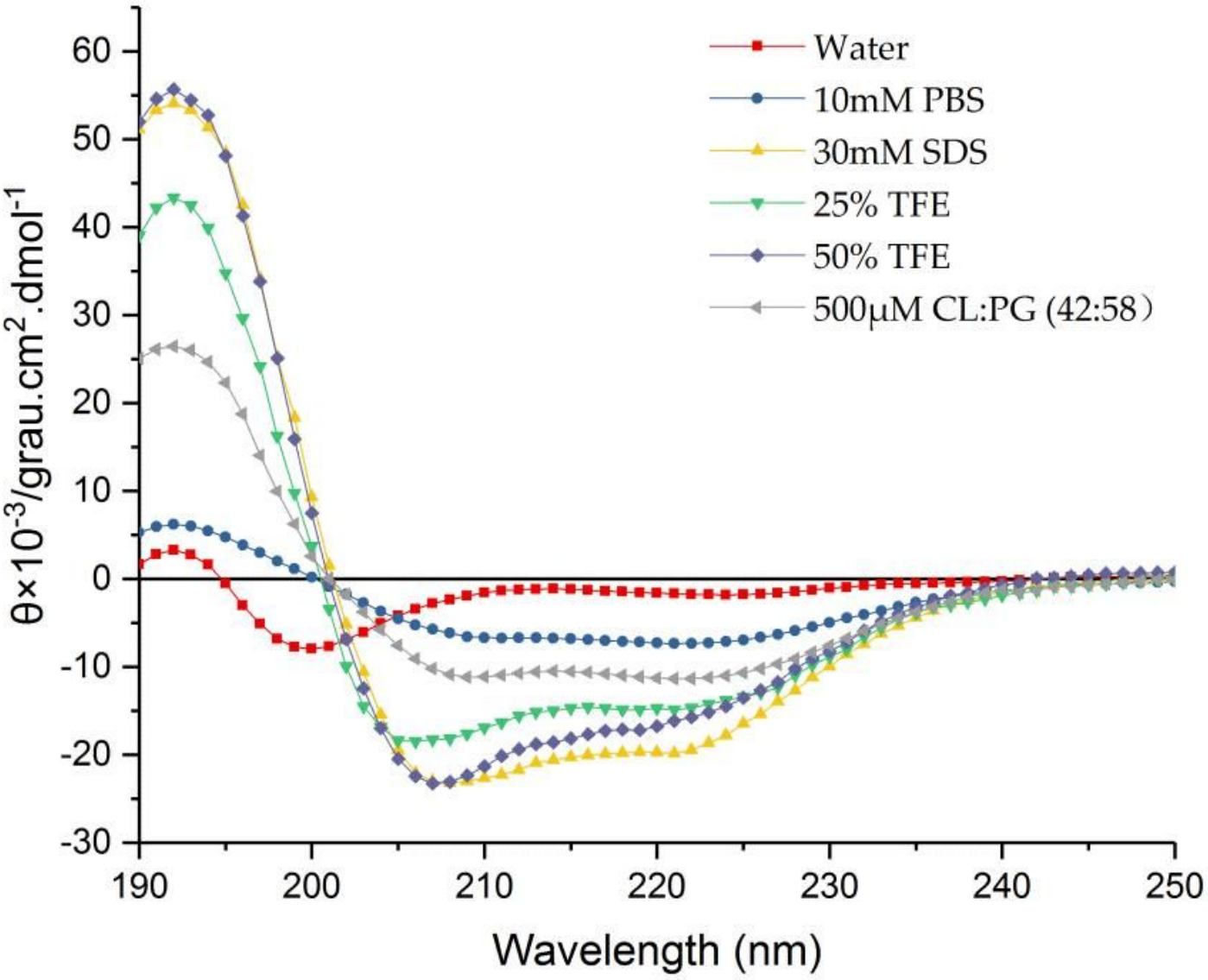

Figure 4

CD spectrum of LHH1. LHH1 was dissolved in water, 10 mM PBS (pH 7.4), 30 mM SDS, 25% TFE, 50% TFE and 500 μM CL:PG (42:58) to reach a final concentration of 100 μM, respectively. Three scans were averaged for each sample.

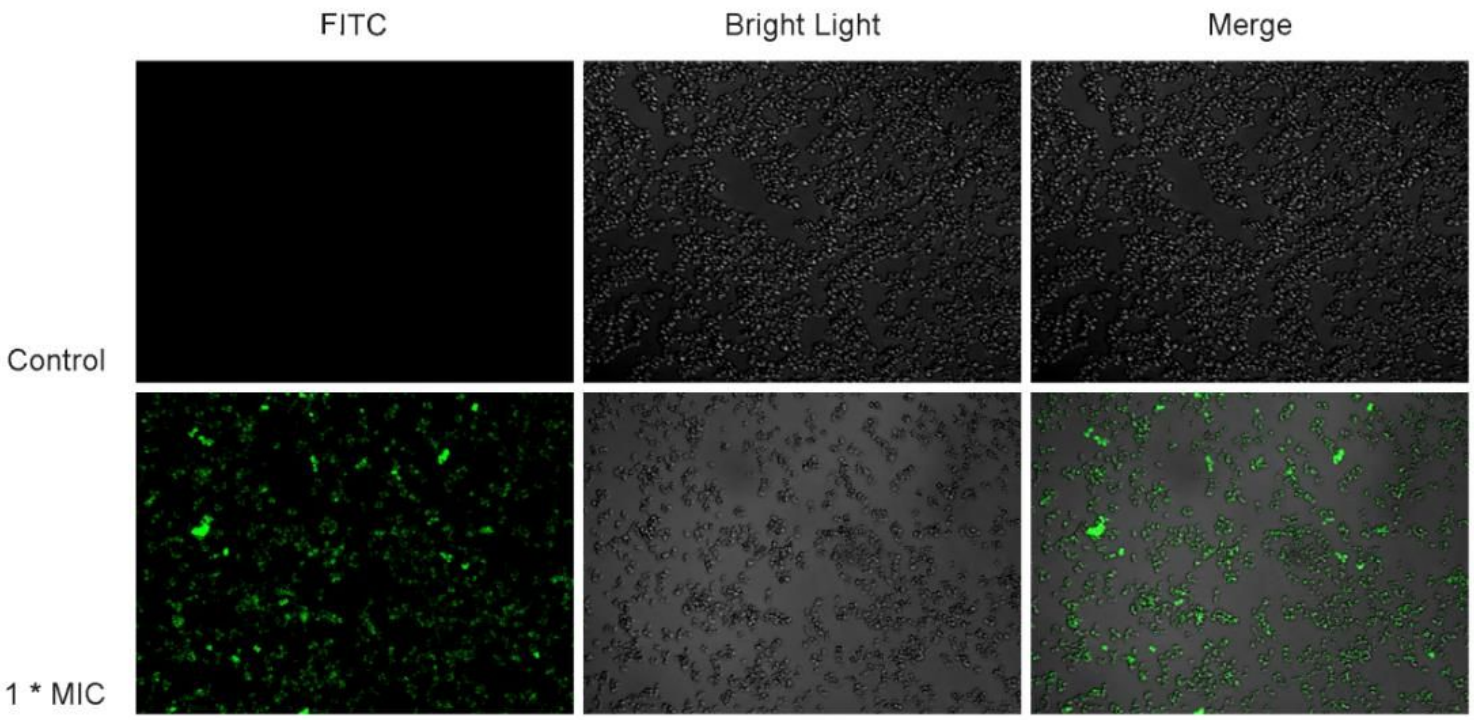

Figure 5

CLSM observation of S. aureus treated with LHH1. S. aureus was co-incubated with 0 or 100 μM FITC-labeled LHH1 for 1 h, and was observed with CLSM.

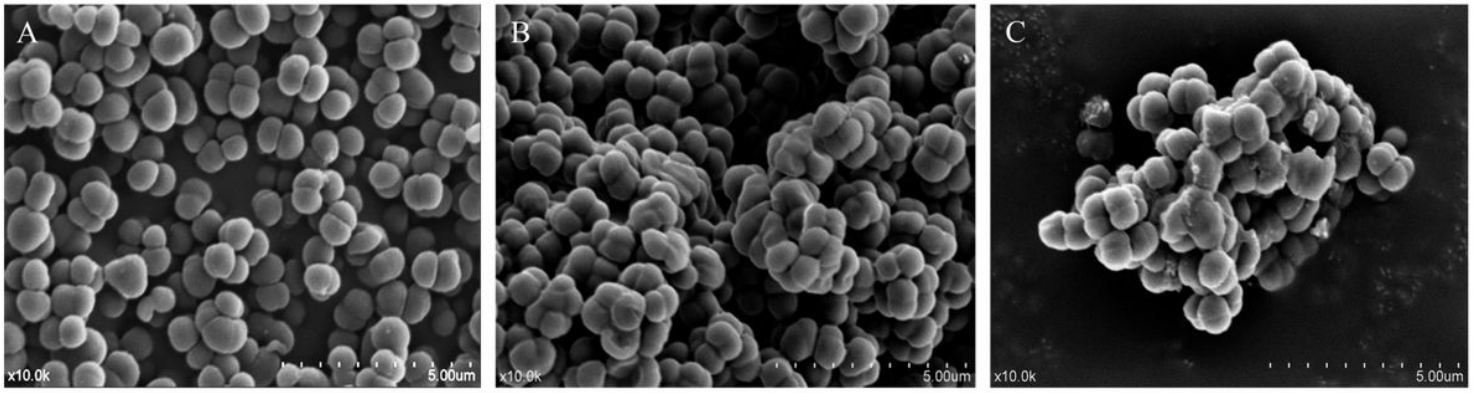

Figure 6

Morphology of S. aureus treated with different concentrations of LHH1. (A) S. aureus was not treated with LHH1; (B) S. aureus treated with LHH1 in 0.5 × MIC; (C) S. aureus treated with LHH1 in 1.0 × MIC.

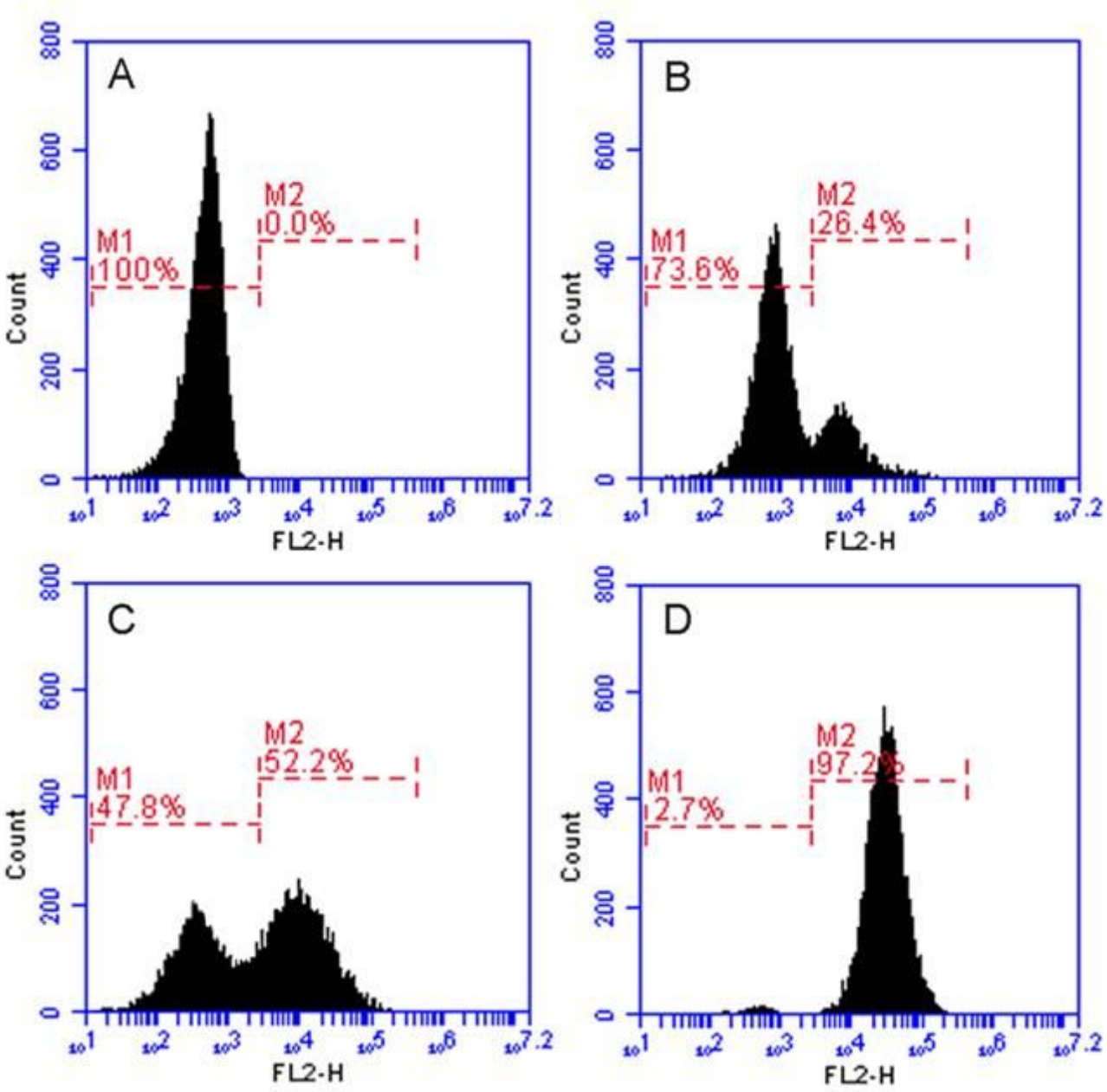

Figure 7

Flow cytometric analysis of the membrane integrity of S. aureus. S. aureus was treated with different concentration of LHH1 at 4 °C for 30 min. (A) S. aureus of control group was treated with 10 mM PBS; (B) S. aureus was treated with LHH1 of 0.5 × MIC; (C) S. aureus was treated with LHH1 of 1.0 × MIC; (D) S. aureus was treated with LHH1 of 2.0 × MIC.

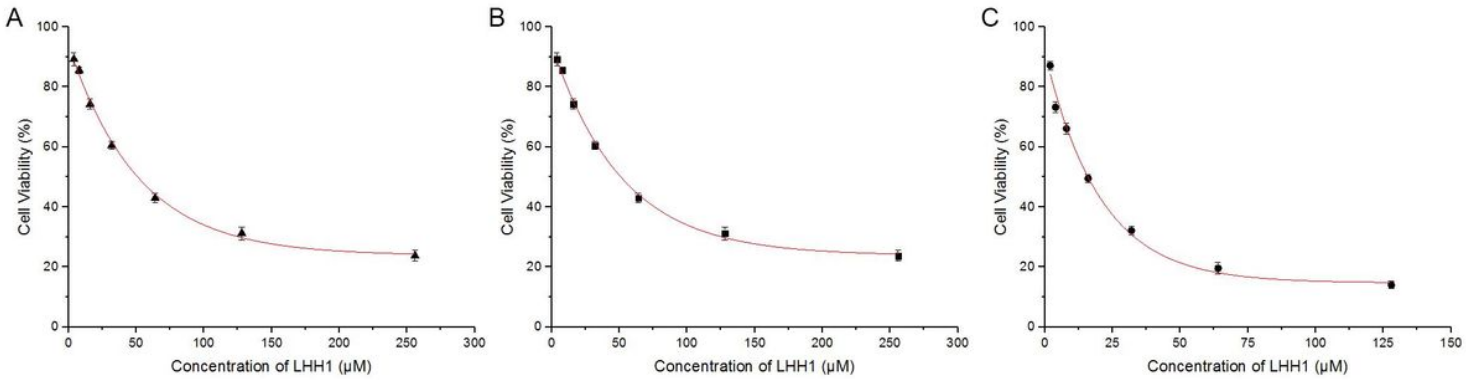

Figure 8

Effect of LHH1 on cell viability of several cancer cells. MGC803 cells (A), HCT116 cells (B) and C666-1 cells (C) were treated with different concentrations of LHH1, respectively.

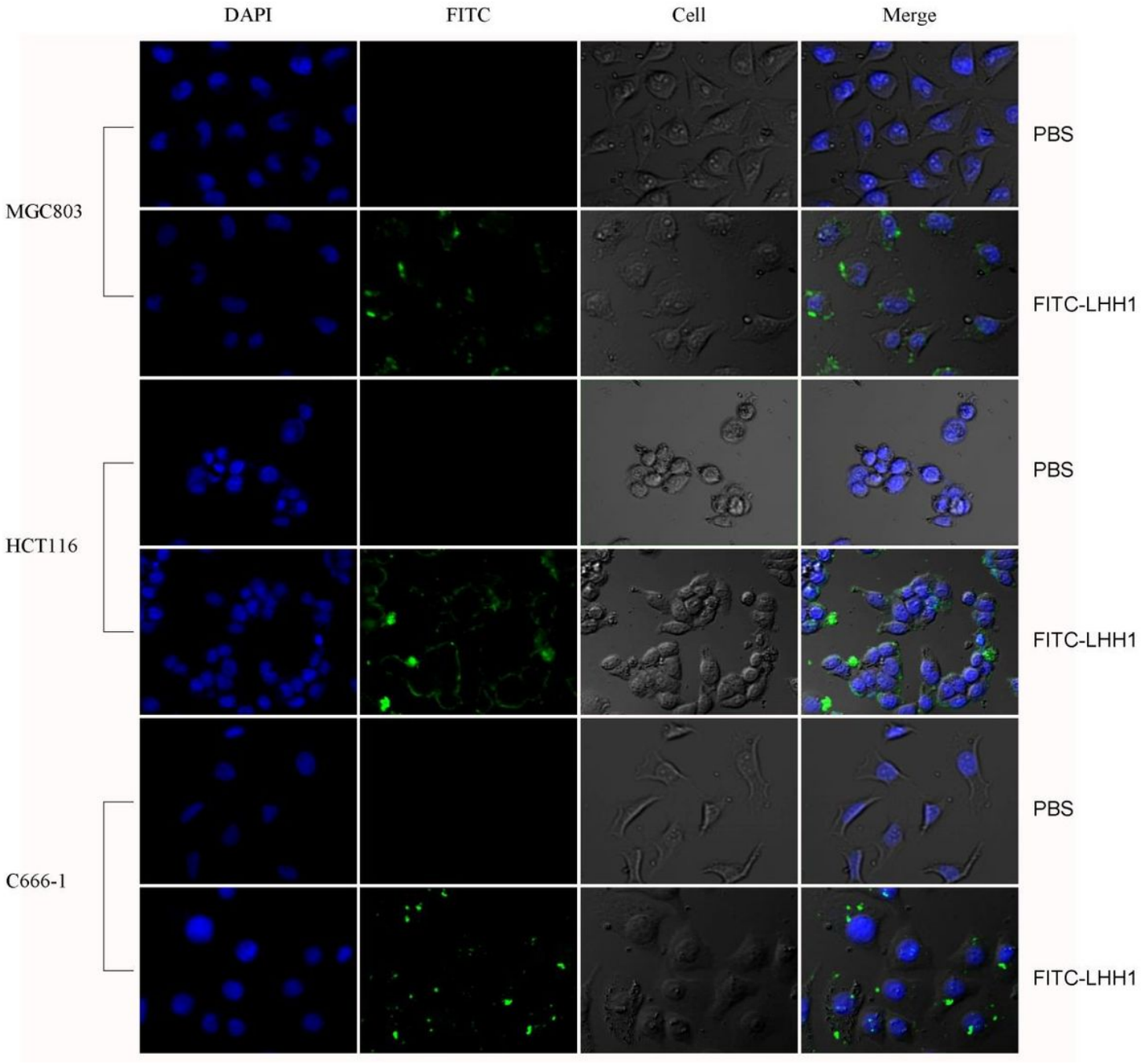

Figure 9

CLSM analysis of membrane destroying effects of LHH1 on cancer cells. The cancer cells were treated with FITC-labeled LHH1 or not and cell nucleus were stained with DAPI.

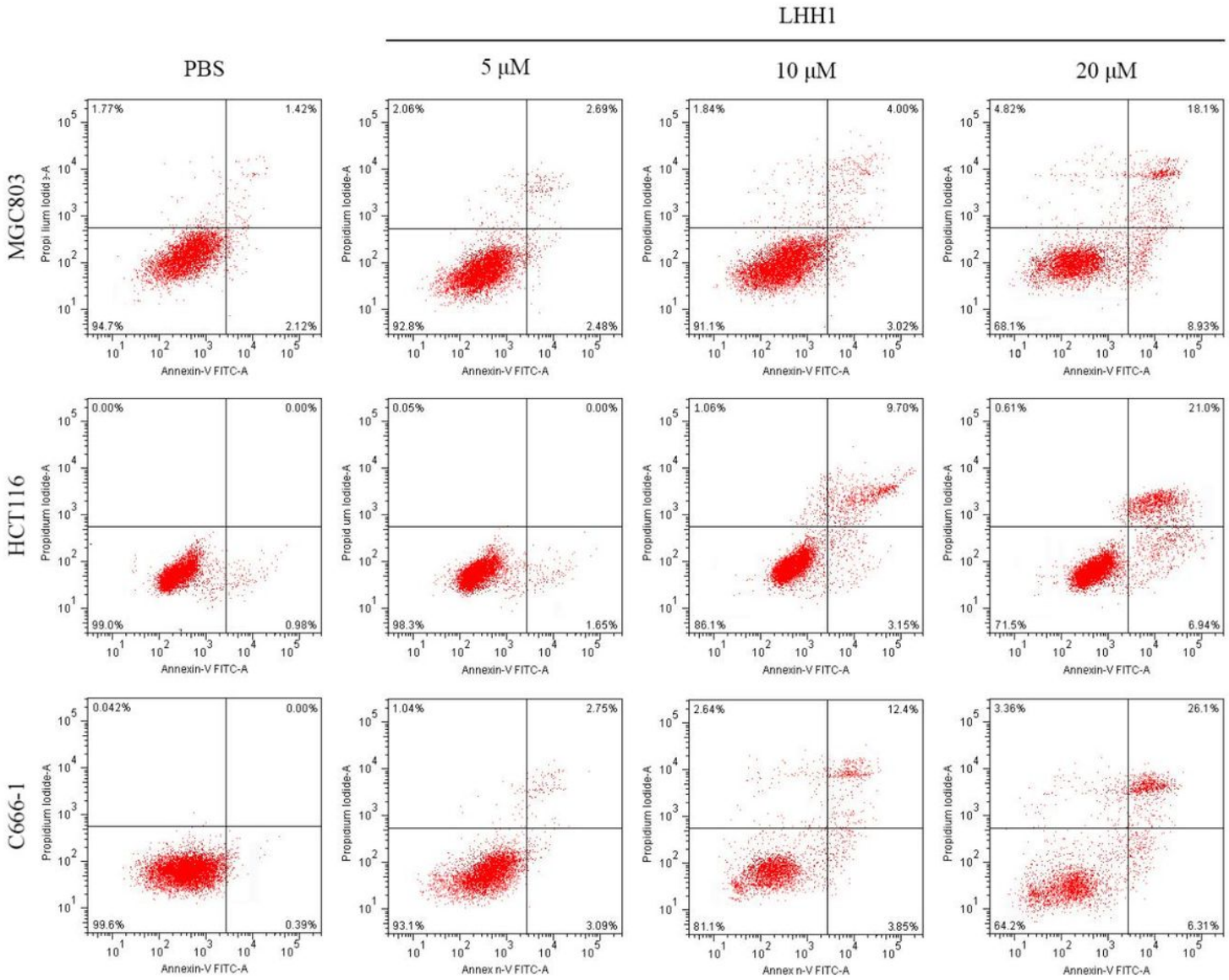

Figure 10

Flow cytometry analysis of apoptosis-promoting effect of LHH1 on cancer cells. The three cancer cells treated with different concentrations of LHH1 (0 μM, 5 μM, 10 μM and 20 μM) were stained with Annexin V-FITC/PI staining.

Figure 11

The sequence similarity alignment.

Supplementary Files

This is a list of supplementary files associated with this preprint. Click to download.

- renamed3d32f.txt
- FigureS11.pdf
- FigureS10.pdf
- FigureS9.pdf
- FigureS8.pdf
- FigureS7.pdf
- FigureS6.pdf
- FigureS5.pdf
- FigureS4.pdf
- FigureS3.pdf
- FigureS2.pdf
- FigureS1.pdf